Influence of profile modifications on the scuffing load capacity of high contact ratio gears

Jaacob Vorgerd[1*], Manuel Joop[2], Peter Tenberge[1]
Ruhr-University Bochum, Germany[1]
Envision Energy CoE GmbH, Germany[2]
jaacob.vorgerd@ruhr-uni-bochum.de, peter.tenberge@ruhr-uni-bochum.de

Abstract: *Scuffing is a spontaneous gear failure mechanism resulting in a disrupted surface. Scuffed gears are more sensitive to dynamic excitation and friction. Besides the lubricant and the material, the scuffing load capacity is mainly dependent on the gear geometry. High contact ratio gears exhibit a lower load carrying capacity due to an increased dissipation of frictional heat in the outer mesh positions. In this paper this phenomenon is addressed with experiments and simulative analysis. Based on these works, recommendations for adequate profile modifications are derived to maximize the load carrying capacity regarding scuffing of high contact ratio gears.*

Keywords*: CYLINDRICAL GEARS, SCUFFING, GEAR FRICTION, FLASH TEMPERATURE, PROFILE MODIFICATION*

1. Introduction

Warm scuffing is a spontaneously occurring, adhesive damage mechanism of highly loaded slide-roll contacts, e.g. in gears [1, 2]. Scuffed surfaces are more sensitive to vibration and exhibit poorer frictional properties. The verification of the scuffing load capacity is often mandatory in the design process of drive systems. With regard to increasing power densities, especially in high-speed electric mobility drives, high contact ratio gears are preferably used. Extending the length of the usable involute leads to improved dynamic properties with lowered excitation of vibrations but it can be more susceptible to scuffing [2–5]. In this paper, experimental and simulative results of a high-speed test rig for cylindrical gears are presented and used to demonstrate the load sensitivity regarding scuffing of high contact ratio gears. Moreover, the influence of profile modification on the local loads during a full gear mesh are shown. On this basis, recommendations for adequate profile modifications to improve the scuffing load capacity are derived.

2. State of the art

2.1 Scuffing of cylindrical gears

In the case of scuffing, contact points weld locally and are immediately torn apart due to the meshing kinematic [6, 7]. The damage that occurs is always found in pairs (pinion/wheel) at the outer mesh positions A or E with characteristic marks in rolling direction [8]. Scuffing is initiated by heat dissipation in the slide-roll contact under the influence of friction [8–10]. Scuffing preferably occurs at contact points with positive slip of the driving pinion, which are located at the tooth tip. The counterparts can be found at the tooth root of the driven wheel (red highlighted mesh positions in **Fig. 1**). For high contact ratio gears it has also been experimentally proven that scuffing occurs in flank areas with negative slip [5, 11, 12].

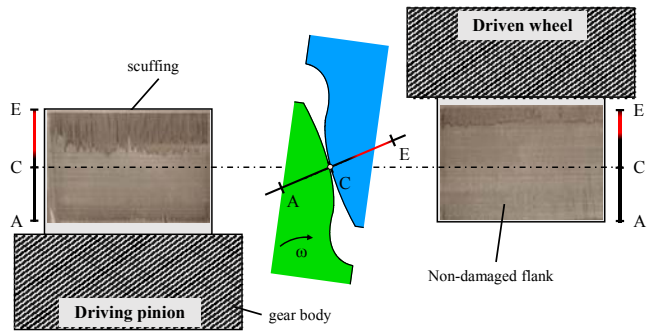

Fig. 1 *Scuffing of cylindrical gear pairs*

The flash temperature method according to Blok [9, 13] has become established as an indicator for scuffing. It is used in the most reputable standards ISO 6336-20 [14] and AGMA 925-A03 [15]. Flash temperatures describe the frictional energy input into the material near the surface below the contact area in the form of a temperature rise. On a macroscopic scale the temperature field extends up to $0.1 \cdot b_H$ into the material depth related to the Hertzian contact width b_H [16]. The maximum temperature is located close to the surface. As an alternative indicator for scuffing, energy criteria are suitable [5, 17]. These criteria additionally consider the local contact time and representing the absorption of thermal energy into the contact points.

2.2 High contact ratio gears

To minimize manufacturing costs for gear hobbing, uniform rack profiles have become established in gear production [2]. Standard rack profiles according to ISO 53 [18] result in a contact ratio of $\varepsilon_\alpha = 1.4 - 1.6$. In view of increasing flexibility in production, it is becoming more and more common to deviate from these standard profiles and design the gear geometry to meet the load condition as required. The dynamic of drive trains is becoming increasingly important, which is why high contact ratio gears with better stiffness properties are used.

High contact ratio gears ($\varepsilon_\alpha = 2.0$) imply the utilization of a larger effective range of the theoretical involute (T_1 to T_2). The resulting gain in contact ratio has a positive effect on the load distribution, but also leads to greater distances between the root or tip mesh positions to the pitch point. Thus, the gear mesh is affected by greater sliding velocities, which leads to a specifically greater dissipation of frictional heat and higher flash temperatures (**Fig. 2**). From a design point of view, the scuffing load capacity of high contact ratio gears can be addressed with suitable profile modifications by relieving the highly loaded contact points close to the edge of the path of contact.

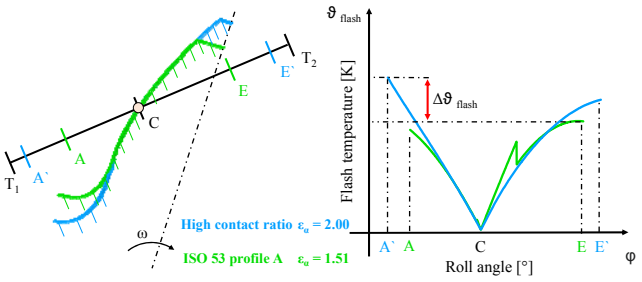

Fig. 2 *Influence of the tooth height on the local scuffing loads*

3. Methodology

3.1 Experiments

The experiments shown in this paper were carried out on a high-speed gear test for investigating the load carrying capacity of cylindrical gears with pitch line velocities up to v_u = 100 m/s. The basic operating principle consists of a back-to-back arrangement of two gearboxes of equal transmission ratios in a closed power loop. The operating principle corresponds to the same as used in conventional gear test rigs according to DIN ISO 14635 [19] but is designed to cover higher speeds.

Fig. 2 shows the schematic layout of the high-speed test rig. In the test gearbox, the test wheelset (2) is thermally insulated by an insulating housing (3). The test gears are injection-lubricated (1) and separated of the bearings without mixing of the lubricating oil circuits. The closed power loop (4) between the test and slave

gearboxes is loaded with torque by a mechanism integrated in the slave wheelset (6). Passing a rotary transmission (8), an axial force is hydraulically applied to the axially shiftable slave wheels (7), resulting in a torque load due to the helix angle. The slave pinions are joint stiff to their shaft. Torque and speed are measured with a torque measuring flange (5). An electric motor (9) feeds in the necessary drive power to maintain the power circuit. **Tab. 1** displays the technical specifications.

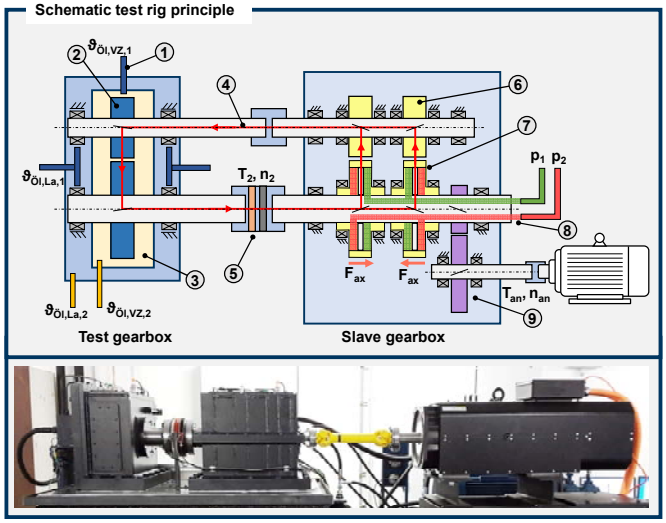

Fig. 3 *Schematic principle of the high-speed test rig (HDP)*

Tab. 1: *Technical specifications of the high-speed test rig (HDP)*

Denomination	Symbol	Unit	Value
Centre distance	a	mm	203.3
Rotational speed pinion shaft	n_1	rpm	up to 12000
Torque load at wheel shaft	T_2	Nm	up to 4000
Circulating mechanical power	P_{mech}	kW	up to 3300
Lubricant temperature	ϑ_{oil}	°C	up to 120

For testing purpose, two gear variants (Variant 1 and Variant 2) with a high contact ratio were used. Both variants differ in their maximum sliding speed due to the choice of the normal module. The profile shift coefficients were designed by balancing the specific sliding velocities at the tip and root mesh positions. Each geometry variant covers two sub-variants of profile modifications. The modification-variant A represents a geometry without a profile modification. For modification-variant B, a tip relief was applied in each case. In terms of materials, the test wheels were made of 18CrNiMo7-6 with a conventional case hardening. After profile grinding, the surface roughness in profile direction was Ra = 0.3 µm (**Tab. 2**).

Tab. 2: *Test gear geometry*

Denomination	Symbol	Unit	Variant 1		Variant 2	
Normal module	m_n	mm	4.50		5.50	
Number of teeth	z_1 / z_2	-	36 / 54		30 / 45	
Face width	b_1 / b_2	mm	22 / 20		22 / 20	
Normal pressure angle	α_n	°	20.00		20.00	
Helix angle	β	°	5.00		5.00	
Profile shift coefficient	x_1 / x_2	-	0.141 / -0.135		-0.060 / -0.568	
Tip circle diameter	d_{a1} / d_{a2}	mm	174.63 / 253.45		176.69 / 253.94	
Profile modification	Modification		A	B	A	B
	C_{a1} / C_{a2}	µm	0.0 / 0.0	22.5 / 22.5	0.0 / 0.0	27.5 / 27.5
	l_{Ca1} / l_{Ca2}	mm	0.0 / 0.0	6.75 / 6.75	0.0 / 0.0	8.25 / 8.25

The test conditions were based on the methodology of the scuffing test acc. to DIN 14635-1 [19] (**Tab. 3**). Operating speeds were varied as part of the project. The torque levels are chosen to correspond with the Hertzian pressure in pitch point. In each load stage, the test gears are loaded for 15 minutes until constant temperature conditions are established. After completion, the flanks are optically inspected for damage and the torque load is increased until the test gears meet the failure criterion described in [19]. To supply lubricant at increased operational speeds, injection lubrication was installed. In the experiments plain mineral oil of viscosity grade ISO VG 68 was used. The lubricant temperature was set to 90 °C.

Tab. 3: *Test conditions*

Denomination	Symbol	Unit	Variant 1	Variant 2
Pitch line velocity	v_u	m/s	20 to 70	20 to 55
Hertzian stress (pitch point)	p_{HC}	MPa	146 to 1841 (12 load stages S_{SKS})	146 to 1841 (12 load stages S_{SKS})
Test duration	-	min	15	15
Lubricant temperature	ϑ_{oil}	°C	90	90
Lubricant	-	-	ISO VG 68 (plain mineral oil)	ISO VG 68 (plain mineral oil)

3.2 Simulation

For the modeling of the loaded gear contacts, a load distribution approach by Walkowiak [20] is used. By taking into account material stiffnesses, the local load and velocity parameters between the start and the end of the contact path can be calculated. This approach also allows to consider profile modifications with respect to local load situations in the outer mesh positions. Based on the local load parameters and the EHL-condition, coefficients of friction are calculated using a model by Löpenhaus [21] (**Eq. 1**).

$$\mu_r = e_1 \cdot v_\Sigma^{e_2} \cdot \exp(e_3 \cdot p_H) \cdot (e_4 \cdot \eta_{oil}^2 + e_5 \cdot \eta_{oil} + e_6) \cdots \cdot Ra^{e_7} \cdot \frac{|sl|}{(|sl| + e_8)^2 + e_9} \cdot \rho_{red}^{-0,2} \cdot X_L \cdot X_{OS} \quad (1)$$

The estimation of scuffing is done by evaluating friction-sensitive load parameters as the flash temperature or the specific contact energy. For calculating local contact temperatures near the surface, a thermal FD-network is used covering a depth of $m_n/50$. The trajectory of the heat source along the involute causes a heat flux to diffuse into the material through the Hertzian contact patterns. Beyond the model approach by Blok, the thermal network can represent temperature-increasing effects due to the meshing kinematic in the outer mesh positions. According to Joop [5], the time-related energy absorption in the Hertzian contact patterns, specific contact energy (**Eq. 2**), is suitable as a model approach for the local scuffing load capacity. The general modeling approach is schematically shown in **Fig. 4**. Further information can be found in [5].

$$E_K = \frac{1}{A_K} \cdot \int_{t_K} \gamma \cdot \mu_r \cdot F_N \cdot |v_g| dt \quad (2)$$

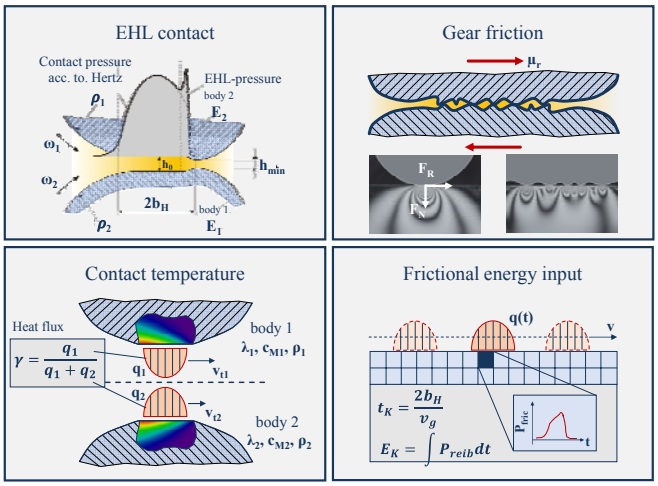

Fig. 4 *Simulation approach to estimate scuffing*

4. Experimental results

The experimental results in **Fig. 5** show that the tooth height influences the scuffing load capacity negatively. A larger tooth height leads to increased relative sliding velocities. In the test points the failure load stage is reduced by approx. 1 – 2 load levels S_{SKS}. In each individual test condition, the profile modification has a positive effect on the load capacity compared to the unmodified reference. Further information on the determination of the failure load stages depending on the damage pattern can be found in [11, 22]. An analysis of the pitch line velocity on the scuffing load capacity can be found in [5, 12].

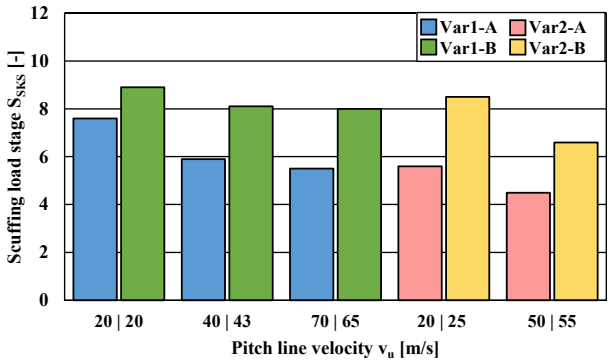

Fig. 5 *Scuffing load capacity of the test points*

Fig. 6 shows a picture of a scuffed pinion flank after the test. The damage pattern is present uniformly along the flank line. In tangential direction the scuffing marks extend from the outer mesh positions close to the pitch point. SEM images of the local damage points confirm the material welding. The welded contact points are torn apart by the meshing kinematics and a worn and fractured surface with an accumulation of small pores appears. In the non-damaged areas, the grinding grooves of the profile grinding process retain.

5. Transfer of the evaluation method

From the experimental results, it is evident that the scuffing-sensitive design of gears with high contact ratio can be compensated by an adequate profile modification. Scuffing is initiated at the outer mesh positions due to overextending the local load carrying capacity. For improving the load carrying capacity the dissipation of frictional heat in these points must be reduced. The simulation model presented allows to calculate the local loads and the influence of the profile modification. The dissipation of frictional heat is mainly dependent on the local tribological load condition of normal force, sliding speed, coefficient of friction and the EHL conditions. In addition, effects such as the stiffness-related extension of the contact time and the engagement kinematics in the outer mesh positions have an impact on scuffing. Using profile modifications, mainly the load distribution can be modified. The sliding velocities, curvatures and the influence on the coefficient of friction are less dependent of the profile modification.

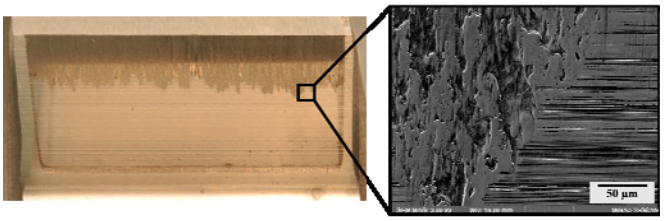

Fig. 6 *Picture of a scuffed gear flank with a close-up SEM image*

To evaluate the scuffing load capacity of various profile modifications, **Fig. 7** shows the local load distribution in form of the contact pressure (a) and the normal force (b), the specific contact energy (c) and the contact temperatures (d) along the path of contact. The path of contact is represented by the involute radius of the driving pinion to indicate the damage location and the effects during the outer meshing positions. For the simulation the basic geometry is identical to variant A. The variants without or less tip relief (variants $C_{a1} = 0$ µm to $C_{a1} = 40$ µm) exhibit large normal forces in the outer meshing positions as well as double rollovers of individuals points, which leads to locally high contact temperatures and frictional loads. On the other hand, the area around the pitch point is less heavily loaded. As the amount of tip relief increases, the normal force is concentrated in the region around the pitch point, which leads to reduced load of the outer mesh positions. The almost linear increase in the contact normal force of the variant $C_{a1} = 80$ µm is desirable here. Lowering the normal forces, results in the scuff-sensitive flank points being relieved in terms of their temperature development. The scuffing load carrying capacity significantly benefits from the profile modified involute. However, the load capacity regarding pitting can decrease due to the higher contact pressure around the pitch point. Ultimately, these two types of stress must be weighed up against each other.

In the design process of profile modifications, it is important to

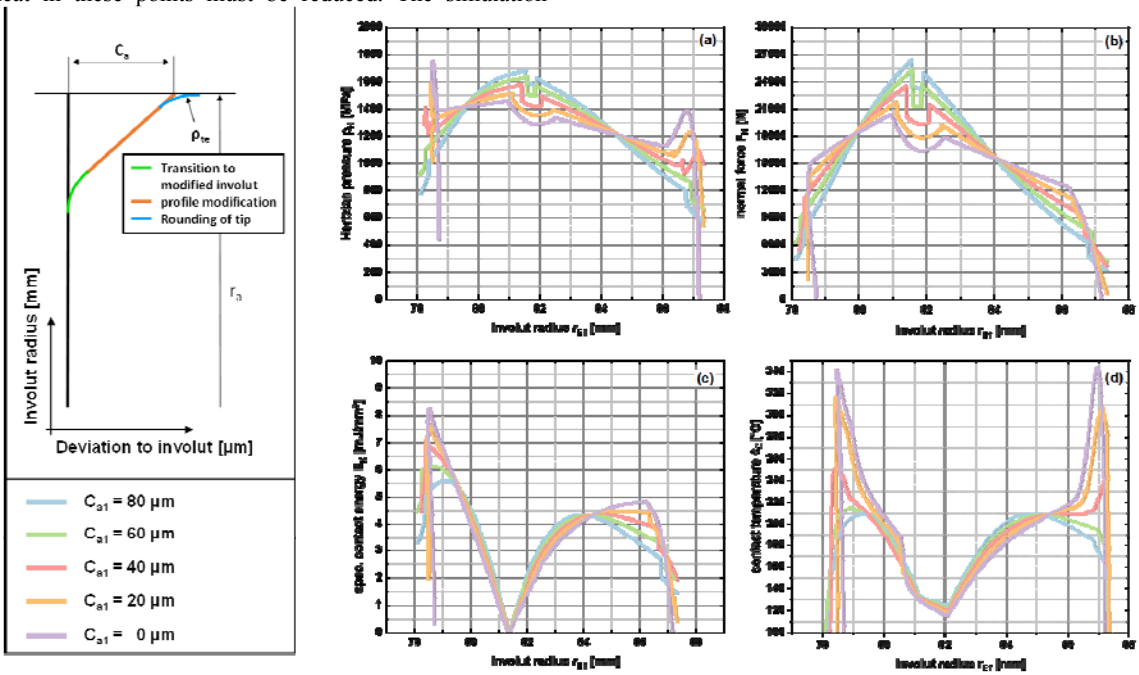

Fig. 7 **Analysis of different profile modifications on the scuffing load carrying capacity**

compensate for elastic tooth deformation so that double rollovers and impulse-like initial engagements do not occur in the outer mesh positions. As a design suggestion, the following strategy can be recommended for high contact ratio gears:

1. The tip relief must fully compensate for the elastic deformation of the tooth pair. Due to the larger tooth height, $C_{a1} = m_n/100$ as an approximate value for the tip relief is recommended to compensate for high loads. The shape of the profile modification (linear, progressive) can be used to improve the actual contact ratio of the lower loaded gear contact. Transition functions between the non-modified involute, the modified involute and the tip rounding also lead to better curvature conditions.
2. The length of the profile modification must be applied so that a smooth load gain during the gear mesh is achieved. In the case of high contact ratio gears, the profile modification extends close to the pitch point.
3. The modification of the flank line relieves the edges of the gear width and compensates for torsional deformations.

6. Discussion

In this article, the influences of high contact ratio gears on their scuffing load capacity are shown. Due to their large tooth height, high contact ratio gears can be more sensitive to scuffing if the profile is not sufficiently modified. In the gear design, it is important to reduce the load in outer mesh positions and thus the dissipation of frictional heat. In the experiments, an increased scuffing load capacity of gears with a tip relief could be determined compared to non-modified gears. Recommendations on the design of profile modifications could be derived based on a simulation model.

The experiments shown were all carried out with plain mineral oil and profile-ground gears. In modern gear applications, cylindrical gears with enhanced surface conditions are increasingly used. In addition, the load-carrying capacity of lubricants can be significantly increased by the addition of additives. In the moderate pitch line velocity range, these effects have already been confirmed experimentally. For the high-speed applications, there is still a need for research to determine whether these improvements in load carrying capacity also hold at higher speeds and under improved EHL-conditions.

7. References

[1] DIN 3979, *Zahnschäden an Zahnradgetrieben*, (1979)
[2] G. Niemann, H. Winter, *Getriebe allgemein, Zahnradgetriebe - Grundlagen, Stirnradgetriebe*, 2. Auflage (2003)
[3] H. Linke, *Stirnradverzahnung: [Berechnung - Werkstoffe - Fertigung]*, 2. Auflage (2010)
[4] P. Hepermann, *Untersuchungen zur Fresstragfähigkeit von Groß-, Schräg- und Hochverzahnungen*, PhD-thesis Ruhr-Universität Bochum (2013)
[5] M. Joop, *Die Fresstragfähigkeit von Stirnrädern bei hohen Umfangsgeschwindigkeiten bis 100 m/s,* PhD-thesis Ruhr-Universität Bochum (2018)
[6] R. W. Snidle, H. P. Evans, *Understanding Scuffing and Micropitting of Gears* (2004)
[7] K. Sommer, R. Heinz, *Verschleiß metallischer Werkstoffe*, 2. Auflage (2014)
[8] K. Michaelis, *Die Integraltemperatur zur Beurteilung der Fresstragfähigkeit von Stirnradgetrieben*, PhD-thesis Technische Universität München (1987)
[9] H. Blok, *Theoretical study of temperature rise at surfaces of actual contact under oiliness lubricating conditions*, Proc. Gen. Disc. Lubric. 2, p. 222–235 (1937)
[10] G. Lechner, *Die Freßlastgrenze bei Stirnrädern aus Stahl*, PhD-thesis Technische Universität München (1966)
[11] M. Joop, H. Ittenson, *Örtliche Fresstragfähigkeit*. Abschlussbericht zu Forschungsvorhaben FVA 598 II (2018)
[12] J. Vorgerd, P. Tenberge, *Scuffing of cylindrical gears with pitch line velocities up to 100 m/s*, Forschung im Ingenieurwesen, Jg. 2 (2021)
[13] H. Blok, *Measurement of temperature flashes on gear teeth under extreme pressure conditions,* Proc. Gen. Disc. Lubric. 2, p. 14–20 (1937)
[14] ISO 6336-20, *Calculation of load capacity of spur and helical gears - Part 20: Calculation of scuffing load - Flash temperature method* (2017)
[15] AGMA 925-A03, *Effect of Lubrication on Gear Surface Distress* (2003)
[16] J.C. Jaeger, H.S. Carslaw, *Conduction of heat in solids*, 2. Edition (1959)
[17] J.O. Almen, *Surface Deterioration of Gear Teeth*, Conference on Mechanical Wear (1948)
[18] ISO 53, *Stirnräder für den allgemeinen und Schwermaschinenbau - Standard-Bezugszahnstangen – Zahnprofile,* (1998)
[19] DIN ISO 14635, *FZG-Prüfverfahren Teil 1 - FZG-Prüfverfahren A/8,3/90 zur Bestimmung der relativen Fresstragfähigkeit von Schmierölen,* (2006)
[20] M. Walkowiak, *Örtliche Belastungen und Verschleißsimulation in den Zahneingriffen profilkorrigierter gerad- und schrägverzahnter Stirnräder zwischen Einfederungsbeginn und Ausfederungsende,* PhD-thesis Ruhr-Universität Bochum (2013)
[21] C. Löpenhaus, *Untersuchung und Berechnung der Wälzfestigkeit im Scheiben- und Zahnflankenkontakt,* PhD-thesis RWTH Aachen (2015)
[22] L. Schlenk, *Untersuchungen zur Fresstragfähigkeit von Großzahnrädern*. PhD-thesis Technische Universität München (1995)

Abbreviations

a	[mm]	Center distance
b	[mm]	Facewidth
b_H	[mm]	Half Hertzian contact width
c_m	[J/kg□K]	heat capacity
d_a	[mm]	Tip circle diameter
e	[-]	Weight parameters
h_0	[µm]	Central EHL fluid film thickness
h_{min}	[µm]	Minimum EHL fluid film thickness
l_{Ca}	[mm]	Length of tip relief
m_n	[mm]	Normal modulus
n_1	[rpm]	Rotational speed
p_H	[MPa]	Hertzian stress
q	[W]	Frictional heat
r_E	[mm]	Involut radius
sl	[-]	Slide-roll ratio (slip)
t_K	[s]	Local contact time
x	[-]	Profile shift coefficient
z	[-]	Number of teeth
v_g	[m/s]	Sliding velocity
v_u	[m/s]	Tangential velocity (pitch point)
v_Σ	[m/s]	Sum velocity
A	[-]	Engagement point of active root circle
A_K	[mm²]	Hertzian contact pattern
C	[-]	Engagement point of pitch circle
C_a	[µm]	Tip relief

E	[-], [GPa]	Engagement point of tip circle, Modulus of elasticity
E_K	[mJ/mm²]	Specific contact energy
F_N	[N]	Normal Force
F_R	[N]	Friction Force
P_{fric}	[W]	Frictional heat
P_{mech}	[W]	Mechanical power
Ra	[µm]	Arith. mean roughness
S_{SKS}	[-]	Failure load Stage
T	[-], [Nm]	Tangent point, Torque
X_L	[-]	Lubricant factor
X_{OS}	[-]	Surface factor
α	[°]	Normal pressure angle
β	[°]	Helix angle
γ	[-]	Heat sharing factor
ε_α	[-]	Contact ratio
η_{oil}	[mPas]	Dynamic viscosity
λ	[-]	Specific fluid film thickness
μ_r	[-]	Coefficient of friction
ρ_{red}	[mm]	Radius of curvature
ϑ_{flash}	[K]	Flash temperature
ϑ_{oil}	[°C]	Oil temperature
ϑ_C	[°C]	Contact temperature

Indizes

1,2 Pinion / wheel